Title: Filamentous structures in skeletal muscle: anchors for the subsarcolemmal space

Authors: Astrid Feinisa Khairani[1, 2], Yuki Tajika[1], Maiko Takahashi[1], Hitoshi Ueno[1], Tohru Murakami[1], Arifin Soenggono[2], Hiroshi Yorifuji[1].

Academic affiliation: 1: Department of Anatomy, Gunma University Graduate School of Medicine, Gunma, Japan, 2: Department of Anatomy, Faculty of Medicine, Universitas Padjadjaran, Bandung, West Java, Indonesia

Corresponding author: Hiroshi Yorifuji, MD, Ph.D

Department of Anatomy, Gunma University Graduate School of Medicine, 3-39-22 Showa-machi, Maebashi, Gunma 371-8511, Japan, TEL: +81-27-220-7912, FAX: +81-27-220-7916, E-mail: yorifuji@gunma-u.ac.jp

Proofs to: Astrid Feinisa Khairani, astrid.khairani@gmail.com

Keywords: cytoskeleton, filamentous anchoring structure, subsarcolemmal space, costameres, actin filament, intermediate filament, transmission electron microscopy

Abstract

In skeletal muscle fibers, intermediate filaments and actin filaments, provide structural support to the myofibrils and the sarcolemma. For many years, it was poorly understood from ultrastructural observations how these filamentous structures were kept anchored. The present study was conducted to determine the architecture of filamentous anchoring structures in the subsarcolemmal space and the intermyofibrils. The diaphragms (Dp) of adult wild type and *mdx* mice (*mdx* is a model for Duchenne muscular dystrophy (DMD)) were subjected to tension applied perpendicular to the long axis of the muscle fibers, with or without treatment with 1% Triton X-100 or 0.03% saponin. These experiments were conducted to confirm the presence and integrity of the filamentous anchoring structures. Transmission electron microscopy (TEM) revealed that these structures provide firm transverse connections between the sarcolemma and peripheral myofibrils. Most of the filamentous structures appeared to be inserted into subsarcolemmal densities, forming anchoring connections between the sarcolemma and peripheral myofibrils. In some cases, actin filaments were found to run longitudinally in the subsarcolemmal space to connect to the sarcolemma or in some cases to connect to the intermyofibrils as elongated thin filaments. These filamentous anchoring structures were less common in the *mdx* Dp. Our data suggest that the transverse and longitudinal filamentous structures form an anchoring system in the subsarcolemmal space and the intermyofibrils.

Introduction

The cytoskeletons of muscle fibers, except those of myofibrils, contain several types of filamentous structures. The three major types of filamentous structures in the cytoskeleton are actin filaments, microtubules and intermediate filaments. Proper organization of these filamentous structures is critical for establishing the internal architecture of muscle fibers, as well as for maintaining the mechanical integration and stability of the myofibrils and the plasma membrane (sarcolemma) [1-4].

The myofibrils, which are key components of skeletal muscle, are composed of sarcomeres. Sarcomeres are repeating units of interdigitating actin (thin filaments) and myosin (thick filaments) [4, 5]. The sarcomeres are laterally attached to the sarcolemma at the costameres [4-6].

Recently, research on the cytoskeletons of skeletal muscle fibers has expanded the definition of costameres. In the earliest report, costameres were recognized as rib-like structures (*costa* is Latin for "rib") overlying the Z lines of nearby myofibrils [6]. Costameres are currently described as having three distinct domains. Two domains run transversely from the peripheral myofibrils to the sarcolemma; Z-domains are linked to the Z disks of peripheral myofibrils, and M-domains are aligned with the M lines of peripheral sarcomeres. L-domains, the third type, run longitudinally [2, 7, 8]. The correlation of L-domains with the internal parts of myofibrils remains unknown [2, 6-15]. The functions of costameres have been reported to include maintaining the internal framework that links peripheral myofibrils to the sarcolemma [1-4, 16-18]. Other functions include the transmission of force and the stabilization of the sarcolemma during the contractile cycle [2, 4-7, 9, 10, 12, 19]. Even though costameres have such important functions, the ultrastructural characteristics of their

components remain poorly understood.

Filamentous structures in the subsarcolemmal and intermyofibrillar spaces have been studied by electron microscopy, and they have been described as anchoring structures [16-21]. Some researchers have also proposed that actin and intermediate filaments could be components of the filamentous anchoring structures. Detailed studies have focused on Z-domains, whereas descriptions of M-domains and L-domains have been limited. Some filamentous structures have also reportedly been observed at subsarcolemmal densities connected to the Z disks of peripheral myofibrils [16, 22, 23]. Subsarcolemmal densities are distinctive electron-dense plaques that occur on the cytoplasmic side of the sarcolemma [16, 22]. Subsarcolemmal densities have been proposed to be associated with costameres, though this association is still under discussion [2, 4-7, 9, 10, 12, 19, 22]. Several other studies have shown that the sarcolemmal regions between the costameres can bulge outwards during muscle contraction, whereas the costameres remain tightly connected to the Z disks of the peripheral myofibrils [1, 2, 16, 19, 22]. These bulges, or "festoons" [4, 5, 19], are indicative of the presence of very firm connections between the sarcolemma and the peripheral myofibrils [4-7, 19].

Recently, some groups have studied the characteristics of costameric molecules [3, 4, 9], but these studies have mainly relied on observations using light microscopy [9]. Immunofluorescence studies have suggested that vinculin, gamma-actin, spectrin and intermediate filament proteins are structural components of costameres and intermyofibrils at the Z disk level [6, 10, 11, 18, 23, 24]. Ultrastructural studies have also been conducted to study the characteristics of costameres. Immunoelectron microscopic studies have indicated that desmin intermediate filaments serve as physical links between myofibrils, especially at Z-domains. These filaments have also

been shown to connect the Z disks of peripheral myofibrils to the sarcolemma through their associations with plectin 1, dystrophin, vinculin, β-synemin, α-dystrobrevin, actin and subsarcolemmal densities [18, 23, 25]. Molecules in the other costameric domains, such as the M-domains and the longitudinal domains, have not yet been identified.

For the filamentous anchoring structures, the complete picture has yet to be elucidated. To uncover the precise spatial relationships of the components of the anchoring structures that connect the sarcolemma to the peripheral myofibrils or intermyofibrils, we conducted ultrastructural analyses of the filamentous anchoring structures in the subsarcolemmal space and the intermyofibrils.

Materials and methods

Animals

C57BL/10ScN mice and *mdx* mice were obtained from the Central Institute for Experimental Animals (Kawasaki, Japan). The mice (2-4 months old) were deeply anesthetized by inhalation of diethyl ether and intraperitoneal injection of pentobarbital. The protocol used in this study was approved by the Animal Care and Experimentation Committee of Gunma University (#10-061).

Muscle preparation

Diaphragm (Dp) muscles from adult wild-type (WT) mice were used as samples without saponin or detergent treatment. After removal, muscles were directly washed in calcium-free rat Ringer's solution (156 mM NaCl, 5.4 mM KCl, 5 mM HEPES (pH

7.4), 10 mM glucose, 5 mM EGTA, 6 mM $MgCl_2$, 0.5 mM NaH_2PO_4) at 4 °C. They were then pinned down for transverse tension treatment [16, 17] and fixed by immersion in 2% paraformaldehyde (PFA), 2.5% glutaraldehyde (GA) and 0.1 M sodium cacodylate buffer (pH 7.3) containing 0.2% tannic acid [2, 6, 7, 9, 10, 12, 23] at 4 °C for 30 minutes to one hour. Samples were trimmed into small blocks and fixed in the same solution at 4 °C overnight. The following day, samples were post-fixed in 1% OsO_4 in the same buffer, and they were block-stained with 1% aqueous uranyl acetate. The samples were embedded in Epon 812. For samples treated with saponin, Dp muscles from WT mice were used. After being pinned down, they were treated with 0.03% saponin in calcium-free rat Ringer's solution containing a protease inhibitor cocktail (1:100; Nacalai Tesque code no. 25955-11, Kyoto, Japan) for 30 minutes at room temperature, then fixed in 2.5% glutaraldehyde (GA) and 0.2% tannic acid in 0.1 M sodium cacodylate buffer (pH 7.3) [23] at 4 °C overnight. For samples treated with detergent, Dp muscles from WT and *mdx* mice were used. These samples were treated with 1% Triton X-100 in calcium-free rat Ringer's solution containing the protease inhibitor cocktail, then fixed in 2.5% glutaraldehyde in 0.1 M sodium cacodylate buffer (pH 7.3) containing 0.2% tannic acid. The remaining steps of the procedure were performed as described above.

Transmission electron microscopy (TEM)

Ultrathin sections were observed using a Hitachi H-800 or JEOL JEM-1010 transmission electron microscope. Filament diameter was measured on printed images at ×50,000 or ×60,000 using a ×7 micrometer eyepiece [26]. Only straight filaments with a distinct margin and little overlying debris were identified and measured.

Results

To reveal the filamentous architecture as transverse and longitudinal anchoring structures in the subsarcolemmal space and the intermyofibrils, we used several treatments of the TEM samples. Transverse tension treatment, with or without 1% Triton X-100 or 0.03% saponin, was used to confirm the existence and integrity of the filamentous structure. Dp was used because it is easier to stretch transversely than other skeletal muscles [16]. Moreover, in *mdx* mice, Dp shows the typical features of muscular dystrophy, including degeneration, fibrosis and severe functional deficit. *mdx* mice are dystrophin-deficient mice that serve as an animal model for Duchenne muscular dystrophy (DMD) [27, 28]. We also used *mdx* mice for comparisons with WT animals.

Ultrastructure of the filaments in the subsarcolemmal space and the intermyofibrils of WT Dp

We found that tension treatment, with or without detergent or saponin, made it possible to observe filamentous anchoring structures in the subsarcolemmal space and the intermyofibrils. Dp samples without transverse tension or detergent (Fig. 1a) failed to show filamentous structures providing anchorage between the sarcolemma and peripheral myofibrils. The subsarcolemmal space was not identifiable because the sarcolemma was closely attached to the peripheral myofibrils. When tension was applied without detergent treatment (Fig. 1b), the subsarcolemmal space was identified between the sarcolemma and peripheral myofibrils. Some filamentous

structures were observed within the subsarcolemmal space. Many membrane organelles of unknown origin remained, most likely because no detergent treatment was applied. Dp samples subjected to 1% Triton X-100 without tension treatment (Fig. 1c) also failed to show filaments. Dp samples with both 1% Triton X-100 and transverse tension treatment (Fig. 1d) yielded better results for the observation of filamentous anchoring structures.

Three independent Dp samples (Figs. 2a-c) were stretched transversely and then fixed without detergent. In these samples, the subsarcolemmal space could be visualized, but organelles of unknown origin obscured the underlying structures and interfered with observation in some locations. The filamentous anchoring structures appeared to survive the transverse tension treatment. Filaments from the same group (Figs. 2a-c) that had less overlying debris and more distinct margins were measured. Higher magnification figures from the boxed areas that illustrated with two white arrows showing a 10-nm space between them are shown to clarify the measuring process of filaments diameter (Figs. 2d-f). The diameter of thin filaments were within the space of two white arrows, while the diameter of intermediate filaments were exceeded. Length between the filaments margins were measured and then calculated to have the value of filament diameter. From the samples (Figs. 2a-c), the diameters of the thin filaments were 8.20 ± 1.16 nm (n = 12) and the 10-nm-filaments were 11.65 ± 1.63 nm (n = 4). Based on the measured diameters, it is highly possible that these thin filaments (8.20 ± 1.16 nm) represent actin filaments. The 10-nm filaments (11.65 ± 1.63 nm) appeared to be intermediate filaments [29]. This interpretation is consistent with previous reports that the costameric cytoskeleton mainly comprises intermediate filaments and actin filaments [3, 4]. Some elongation of the thin filaments was apparent in both the subsarcolemmal space and the intermyofibrils. As

reported previously, subsarcolemmal densities can sometimes be observed at the membrane level at attachment sites of the filamentous systems from the Z lines or M lines of peripheral myofibrils [16, 22]. Most actin filaments were found to be inserted into these subsarcolemmal densities. Transverse sections of Dp samples treated in the same manner (Figs. 3a, b) confirmed the appearance of the filamentous anchoring structures that connect the sarcolemma to peripheral myofibrils. Thin filaments (8.29 ± 0.55 nm; n = 11) were clearly visible originating from the A-band, and some filaments stretched from the I-band to the sarcolemma. As seen in longitudinal sections (Figs. 2a-c), these thin filaments may represent actin filaments. They appear to make direct contact with the subsarcolemmal densities.

To ensure the presence and integrity of the filamentous structures, three independent samples of Dp (Figs. 4a-c) were treated with transverse tension and 1% Triton X-100. The subsarcolemmal space was clearly exposed. Higher magnification figure showed that the diameter of thin filament was less than the 10-nm space of the two white arrows, while the diameter of intermediate filament was exactly filled the space (Figs. 4d). The filamentous structures, including actin filaments (8.23 ± 0.44 nm; n = 9) and intermediate filaments (10.38 ± 0.52 nm; n = 8), formed firm transverse connections between the sarcolemma and the Z disks and M lines of peripheral myofibrils. Most of the longitudinal structures were elongated thin filaments. Some subsarcolemmal densities were observed, especially above the Z disk and M line areas. Membrane organelles of unknown origin were less common but still present. The persistent appearance of firm anchoring structures, despite treatment with 1% Triton X-100 and the application of transverse tension, made it clear that the filamentous structures are transverse and longitudinal anchoring structures that connect the sarcolemma to peripheral myofibrils.

Transverse and longitudinal filamentous structures were also present in Dp samples treated with 0.03% saponin and transverse tension (Figs. 5a, b). Those filamentous structures could be identified in longitudinal sections (Fig. 5a) and in transverse sections (Fig. 5b). Actin filaments (7.69 ± 0.33 nm; $n = 8$) and intermediate filaments (10.00 ± 0.50 nm; $n = 7$) were clearly visible in the sections, and they formed transverse connections between the sarcolemma and the Z disks. The longitudinal structures appeared as elongated thin filaments that were mainly located in the intermyofibrils. The insertion of some actin filaments into subsarcolemmal densities was also observed.

Loss of filamentous architecture in the M line domain in *mdx* Dp

We demonstrated that treatment with transverse tension and 1% Triton X-100 or 0.03% saponin allows observation of the filamentous anchoring structures in the subsarcolemmal space and intermyofibrils (Figs. 4 and 5). In the next set of experiments, we used *mdx* mice to determine whether particular ultrastructural features of the anchoring system were affected by these treatments.

Samples of *mdx* Dp [Fig. 6a, b (insert)] were treated with transverse tension and 1% Triton X-100. As with the WT Dp samples that received the same treatment, the subsarcolemmal space was clearly exposed. However, there were differences in the appearance of the filamentous anchoring structures. There were fewer filamentous structures in the *mdx* Dp. Connections between the M lines and the sarcolemma were barely observed. Some 10-nm filaments were present above the Z disk areas.

Discussion

In this study, we provide morphological evidence of filamentous anchoring structures in the subsarcolemmal space and intermyofibrils. The filamentous anchoring structures discussed here are applied to the transverse and longitudinal filamentous structures that appear in the three costameric domains and the intermyofibrils. These filamentous structures can survive treatment with transverse tension and 1% Triton X-100 or 0.03% saponin. Moreover, these structures are able to connect the peripheral myofibrils to the sarcolemma or intermyofibrils (Figs. 4 and 5). Functionally, these lateral linkages would help individual muscle fibers avoid disruptive contraction and would aid in the generation of force [7, 18, 19].

Because our ultrastructural evidence for filamentous anchoring structures in the subsarcolemmal space and intermyofibrils was obtained by electron microscopy of intact muscle treated with Triton X-100 or saponin, we must consider the possibility that these procedures may introduce artifacts, such as filament redistribution or superimposition onto the subsarcolemmal space, Z disks or M lines. A classic experiment by Pierobon-Bormioli demonstrated that muscle framework is difficult to preserve [16]. However, our results, which were obtained from several independent mice and several different treatments, suggest that the observed filamentous anchoring structure distribution was not artifactual. First, Dp samples with no transverse tension or detergent treatment (Fig. 1a) failed to show filamentous structures because the subsarcolemmal space could not be visualized. Second, when tension was applied without detergent treatment (Fig. 1b), some filamentous structures could be observed within the subsarcolemmal space, but the presence of many membrane organelles interfered with observation. Third, Dp samples subjected

to 1% Triton X-100 treatment but not tension treatment (Fig. 1c) also failed to show filaments. Fourth, Dp samples treated with both 1% Triton X-100 and transverse tension (Fig. 1d) yielded better results for the observation of filamentous anchoring structures. Treatment with only transverse tension or transverse tension treatment combined with 1% Triton X-100 or 0.03% saponin (Figs. 2, 4, 5) enabled observation of the filamentous anchoring structures in the subsarcolemmal space and intermyofibrils. These findings are in agreement with previous studies [6, 10, 16-24], and we have obtained new evidence that provides a more comprehensive understanding of the filamentous anchoring structures.

Based on the present and previous data, filamentous anchoring structures in the subsarcolemmal space may be depicted, as shown in Fig.7. Transverse anchoring filamentous structures that laterally interlink the Z disks and M lines of peripheral myofibrils to the sarcolemma were clearly visible, and they were composed of actin and intermediate filaments (Figs. 2-5). By measuring the filament diameters, we confirmed that actin filaments and intermediate filaments are the most likely candidates for linking peripheral myofibrils to the cytoplasmic surface of the sarcolemma [1, 3, 4, 7, 9]. The possibilities that the filamentous anchoring structures were also composed of membrane skeleton protein, such as dystrophin and/or spectrin are low because these molecules are thinner than actin filament [30, 31]. At the Z-domains of costameres, actin and intermediate filaments appeared to cooperate to attach the Z disks of peripheral myofibrils to the sarcolemma (Figs. 4a, 4c, 5a). Actin filaments in particular seem to take the form of longitudinal anchoring structures or elongated filaments, not only in the subsarcolemmal space (Figs. 2-5) but also in the intermyofibrils (Figs. 2 and 5). This result supports the findings of previous immunofluorescence studies, which indicated that costameric actin filaments and

intermediate filaments serve as structural components of both costameres and intermyofibrils at the level of Z lines [10, 18, 23, 24]. Different from the Z-domains, our findings at the M-domains of costameres suggest that only intermediate filaments form the connections between the M lines of peripheral myofibrils and the sarcolemma (Figs. 2b, 4a, 4b). This result is in accordance with previous reports [2, 3, 19, 32]. In the later researches, not only desmin [2, 18, 23, 25] but also keratin filaments [2, 3, 8, 12], are the types of intermediate filaments that are being proposed as anchoring structures between sarcolemma and peripheral myofibril. Desmin enriched at the Z-domains of costameres [2, 3], but was not present in significant amounts at M-domains or L-domains of costameres [7]. The other type is composed of keratin filaments containing keratin 8 (K8) and keratin 19 (K19) [3, 8]. Although keratins are present in smaller amounts than desmin, K8 and K19 are found at both the Z-domains and M-domains of costameres [8, 12]. Our ultrastructural findings ascertained the previous reports by clearly showing that the intermediate filaments are component of filamentous anchoring structures between sarcolemma and peripheral myofibrils.

We were able to visualize the elongation of thin filaments in the subsarcolemmal spaces and in the intermyofibrils (Figs. 2-5). The path of elongation of thin filaments from the peripheral myofibrils to the sarcolemma was clearly demonstrated by our data. This information was lacking in previous studies by Bard and Franzini-Armstrong [17]. Those authors suggested that peripheral filaments are composed of actin and are anchored to Z lines [17], which is consistent with our results. In the subsarcolemmal space, the elongated thin filaments obliquely arose from the peripheral myofibrils and then longitudinally extended before finally inserting into the subsarcolemmal densities (Figs 2-5). Based on this evidence, it is

possible that these elongated thin filaments extending from the peripheral myofibrils to the sarcolemma are actually the ultrastructural L-domains of the costameres.

In Figures 2-5, we also observed the appearance of electron-dense plaques on the cytoplasmic side of the sarcolemma. These plaques are most likely subsarcolemmal densities, as reported previously by Pierobon-Bormioli [16] and Shear [22]. Membrane skeleton proteins such as vinculin [6, 10, 22], dystrophin and β-spectrin [11] are considered to be components of subsarcolemmal densities. From our results, the subsarcolemmal densities appeared in all three domains of costameres. We clearly visualized the association of subsarcolemmal densities with the filamentous anchoring structures, particularly the elongated thin filaments coming from the peripheral myofibrils (Figs. 2, 3, 5). These results remind us of a previous study that mentioned the relationship of subsarcolemmal densities with extracellular structures [22]. In 1985, Shear observed that the densities were associated with extracellular thin filaments that extend from the sarcolemma through the basal lamina [22]. Our observations complete the picture by revealing that the subsarcolemmal densities are also associated with filamentous anchoring structures from the peripheral myofibrils. This association might play a role in anchoring the sarcolemma to the peripheral myofibrils. Thus, we propose that subsarcolemmal densities and their associated filamentous anchoring structures constitute the ultrastructural representation of costameres.

Previous experiments suggest that costameres may serve to laterally transmit contractile forces from the sarcomeres across the sarcolemma to the extracellular matrix, ultimately transmitting the force to neighboring muscle cells [9, 10, 19]. Dystrophin and its associated proteins are found at the sarcolemma in association with the Z-domains of costameres [33, 34]. Confocal immunofluorescence analysis showed

that dystrophin forms a strong mechanical attachment to the sarcolemma [24, 33]. Immunoelectron microscopy revealed that dystrophin distributed close to the cytoplasmic surface of the plasma membrane [35, 36]. In muscle fibers skinned with Triton X-100, immunoelectron microscopy labeled dystrophin at outer-side surface of subsarcolemmal densities [23]. Freeze-fracture replica immunoelectron microscopy showed that labeling of spectrin and dystrophin were at the cytoplasmic surface of the plasma membrane [37]. Dystrophin in the subsarcolemmal densities is associated with integral membrane proteins such as β-dystroglycans [3, 24, 38, 39]. These proteins interaction are associated subsequently with suprasarcolemmal α-dystroglycans, forming a structural links in the sarcolemma and with the basal lamina by binding laminin-2 [23, 39, 40]. On the other hand, dystrophin do not make filaments between sarcolemma and sarcomeres. Dystrophin links to the sarcomeres through other proteins interaction, such as gamma-actin filaments [3, 24]. Our results showed that the subsarcolemmal densities still remained after tension treatment. Thus, dystrophin, spectrin, and other associated proteins might still retained in the densities. DMD is caused by mutations in the gene encoding dystrophin [41-43]. The *mdx* mouse, which is an animal model for DMD, carries a mutation in the dystrophin gene and lacks the native protein [28, 44]. When dystrophin is absent, the link between the costamere and sarcolemma is disrupted, resulting in compromised sarcolemmal integrity [9]. This study provides the first ultrastructural evidence showing the differences between the filamentous anchoring structures of WT and *mdx* Dp samples subjected to the same treatment (Figs. 4 and 6). There were fewer filamentous anchoring structures in the *mdx* Dp samples. Especially connections between the M lines and the sarcolemma were barely observed in the *mdx* samples. Our data support previous studies that found that the M line domains of the costameres are more susceptible to disruption in

mdx mice [2, 11, 13]. The absence of dystrophin and the destabilization of the filamentous anchoring structures may cause the costamere abnormalities observed in *mdx* mice [7, 9, 24, 45].

Taken together, the data from this study show that tension treatment, with or without detergent or saponin treatment, allows observation of the filamentous anchoring structures in the subsarcolemmal and intermyofibrillar spaces. Actin and intermediate filaments show their presence and integrity as components of the transverse and longitudinal anchoring structures in the subsarcolemmal space and the intermyofibrils.

Conclusion

We showed that the transverse and longitudinal anchoring structures along with the subsarcolemmal densities and elongated thin filaments in the subsarcolemmal space might represent the ultrastructural components of the costamere. We also reported a lack of filamentous anchoring structures in *mdx* mice. The mechanism underlying how these structures were lost was not revealed in this study. Further study of *mdx* mice may provide new insights into cytoskeleton organization in skeletal muscle fibers and may contribute to a more comprehensive understanding of how defects cause membrane fragility and muscle wasting.

Acknowledgments

We thank H. Matsuda, M. Shikada and Y. Morimura for both technical and secretarial assistance. This work was supported in part by Grants-in-Aid for Scientific Research from the Ministry of Education, Culture, Sports, Science and Technology of Japan, KAKENHI Grant Numbers 20590183, 23590230.

References

1. Ramaekers FCS, Bosman FT (2004) The cytoskeleton and disease. J Pathol 204:351–354

2. O'Neill A, Williams M, Resneck WG, Milner DJ, Capetanaki Y, Bloch RJ (2002) Sarcolemmal Organization in Skeletal Muscle Lacking Desmin: Evidence for Cytokeratins Associated with the Membrane Skeleton at Costameres. Mol Biol Cell 13:2347–2359

3. Capetanaki Y, Bloch RJ, Kouloumenta A, Mavroidis M, Psarras S (2007) Muscle intermediate filaments and their links to membranes and membranous organelles. Exp Cell Res 313:2063–2076

4. Kee AJ, Gunning PW, Hardeman EC (2009) Diverse roles of the actin cytoskeleton in striated muscle. J Muscle Res Cell Motil 30:187–197

5. Clark KA, McElhinny AS, Beckerle MC, Gregorio CC (2002) Striated Muscle Cytoarchitecture: An Intricate Web of Form and Function. Annu Rev Cell Dev Biol 18:637–706

6. Pardo JV, Siliciano JD, Craig SW (1983) A vinculin-containing cortical lattice in skeletal muscle: transverse lattice elements (“costameres”) mark sites of attachment between myofibrils and sarcolemma. Proc Natl Acad Sci USA 80:1008–1012

7. Bloch RJ, Gonzales-Serratos H (2003) Lateral Force Transmission Across Costameres in Skeletal Muscle. Exerc Sport Sci Rev 31:73–78

8. Ursitti JA, Lee PC, Resneck WG, McNally MM, Bowman AL, O'Neill A, Stone MR, Bloch RJ (2004) Cloning and characterization of cytokeratins 8 and 19 in adult rat striated muscle. Interaction with the dystrophin glycoprotein complex. J Biol Chem 279:41830–41838

9. Ervasti JM (2003) Costameres: the Achilles' Heel of Herculean Muscle. J Biol Chem 278:13591–13594

10. Craig SW, Pardo JV (1983) Gamma Actin, Spectrin, and Intermediate Filament Proteins Colocalize with Vinculin at Costameres, Myofibril-to-Sarcolemma Attachment Sites. Cell Motil 3:449–462

11. Porter GA, Dmytrenko GM, Winkelmann JC, Bloch RJ (1992) Dystrophin colocalizes with β-spectrin in distinct subsarcolemmal domains in mammalian skeletal muscle. J Cell Biol 117:997–1005

12. Stone MR, O'Neill A, Lovering RM, Strong J, Resneck WG, Reed PW, Toivola DM, Ursitti JA, Omary MB, Bloch RJ (2007) Absence of keratin 19 in mice causes skeletal myopathy with mitochondrial and sarcolemmal reorganization. J Cell Sci 120:3999–4008

13. Williams MW, Bloch RJ (1999) Extensive but coordinated reorganization of the membrane skeleton in myofibers of dystrophic (mdx) mice. J Cell Biol 144:1259–1270

14. Williams MW, Resneck WG, Bloch RJ (2000) Membrane skeleton of innervated and denervated fast- and slow-twitch muscle. Muscle Nerve 23:590–599

15. Williams MW, Resneck WG, Kaysser T, Ursitti JA, Birkenmeier CS, Barker JE, Bloch RJ (2001) Na, K-ATPase in skeletal muscle: two populations of β-spectrin control localization in the sarcolemma but not partitioning between the sarcolemma and the transverse tubules. J Cell Sci 114:751–762

16. Pierobon-Bormioli S (1981) Transverse sarcomere filamentous systems: "Z- and M-cables." J Muscle Res Cell Motil 2:401–413

17. Bard F, Franzini-Armstrong C (1991) Extra actin filaments at the periphery of skeletal muscle myofibrils. Tissue Cell 23:191–197

18. Hijikata T, Murakami T, Imamura M, Fujimaki N, Ishikawa H (1999) Plectin is a linker of intermediate filaments to Z-discs in skeletal muscle fibers. J Cell Sci 112:867–876.

19. Street SF (1983) Lateral Transmission of Tension in Frog Myofibers: A Myofibrillar Network and Transverse Cytoskeletal Connections Are Possible Transmitters. J Cell Physiol 114:346–364

20. Garamvölgyi N (1965) Inter-Z bridges in the flight muscle of the bee. J Ultrastruct Res 13:435–443

21. Wang K, Ramirez-Mitchell R (1983) A network of transverse and longitudinal intermediate filaments is associated with sarcomeres of adult vertebrate skeletal muscle. J Cell Biol 96:562–570

22. Shear CR, Bloch RJ (1985) Vinculin in subsarcolemmal densities in chicken skeletal muscle: localization and relationship to intracellular and extracellular structures. J Cell Biol 101:240–256

23. Hijikata T, Murakami T, Ishikawa H, Yorifuji H (2003) Plectin tethers desmin intermediate filaments onto subsarcolemmal dense plaques containing dystrophin and vinculin. Histochem Cell Biol 119:109–123

24. Rybakova IN, Patel JR, Ervasti JM (2000) The dystrophin complex forms a mechanically strong link between the sarcolemma and costameric actin. J Cell Biol 150:1209–1214

25. Hijikata T, Nakamura A, Isokawa K, Imamura M, Yuasa K, Ishikawa R, Kohama K, Takeda S, Yorifuji H (2008) Plectin 1 links intermediate filaments to costameric sarcolemma through β-synemin, α-dystrobrevin and actin. J Cell Sci 121:2062–2074

26. Yorifuji H, Hirokawa N (1989) Cytoskeletal architecture of neuromuscular

junction: localization of vinculin. J Electron Microsc Tech 12:160–171

27. Stedman HH, Sweeney HL, Shrager JB, Maguire HC, Panettieri RA, Petrof B, Narusawa M, Leferovich JM, Sladky JT, Kelly AM (1991) The mdx mouse diaphragm reproduces the degenerative changes of Duchene muscular dystrophy. Nature 352:536–539

28. Ishizaki M, Suga T, Kimura E, Shiota T, Kawano R, Uchida Y, Uchino K, Yamashita S, Maeda Y, Uchino M (2008) Mdx respiratory impairment following fibrosis of the diaphragm. Neuromuscul Disord 18:342–348

29. Ishikawa H, Bischoff R, Holtzer H (1968) Mitosis and intermediate-sized filaments in developing skeletal muscle. J Cell Biol 38:538–555

30. Cohen CM, Tyler JM, Branton D (1980) Spectrin-actin associations studied by electron microscopy of shadowed preparations. Cell 21:875–883

31. Pons F, Augier N, Heilig R, Léger J, Mornet D, Léger JJ (1990) Isolated dystrophin molecules as seen by electron microscopy. Proc Natl Acad Sci USA 87:7851–7855.

32. Lazarides E (1980) Intermediate filaments as mechanical integrators of cellular space. Nature 283:249–256

33. Straub V, Bittner RE, Léger JJ, Voit T (1992) Direct visualization of the dystrophin network on skeletal muscle fiber membrane. J Cell Biol 119:1183–1191

34. Goldstein JA, McNally EM (2010) Mechanisms of muscle weakness in muscular dystrophy. J Gen Physiol 136:29–34

35. Cullen MJ, Walsh J, Nicholson LVB, Harris JB (1990) Ultrastructural localization of dystrophin in human muscle by using gold immunolabelling. Proc R Soc Lond B Biol Sci 240:197–210.

36. Harris JB, Cullen MJ (1992) Ultrastrucutral localization and the possible role of dystrophin. In: Kalkulas BA, Howell JM, Roses AD (eds) Duchenne muscular dystrophy: animal models and genetic manipulation. Raven Press, New York, pp 19–40.

37. Stevenson SA, Cullen MJ, Rothery S, Coppen SR (2005) High-resolution en-face visualization of the cardiomyocyte plasma membrane reveals distinctive distributions of spectrin and dystrophin. Eur J Cell Biol 84:961–971.

38. Jung D, Yang B, Meyer J, Chamberlain JS, Campbell KP (1995) Identification and characterization of the dystrophin anchoring site on β-dystroglycan. J Biol Chem 270:27305–27310

39. Ervasti JM, Campbell KP (1993) A role for the dystrophin-glycoprotein complex as a transmembrane linker between laminin and actin. J Cell Biol 122:809–823.

40. Ibraghimov-Beskrovnaya O, Ervasti JM, Leveille CJ, Slaughter CA, Sernett SW, Campbell KP (1992) Primary structure of dystrophin-associated glycoproteins linking dystrophin to extracellular matrix. Nature 355:696–702.

41. Hoffman EP, Kunkel LM (1989) Dystrophin abnormalities in Duchenne/Becker muscular dystrophy. Neuron 2:1019–1029

42. Campbell KP (1995) Three muscular dystrophies: loss of cytoskeleton-extracellular matrix linkage. Cell 80:675–679

43. O'Brien KF, Kunkel LM (2001) Dystrophin and muscular dystrophy: past, present, and future. Mol Genet Metab 74:75–88

44. Law DJ, Allen DL, Tidball JG (1994) Talin, vinculin and DRP (utrophin) concentrations are increased at mdx myotendinous junctions following onset of necrosis. J Cell Sci 107:1477–1483

45. Bellin RM, Huiatt TW, Critchley DR, Robson RM (2001) Synemin May Function to Directly Link Muscle Cell Intermediate Filaments to Both Myofibrillar Z lines and Costameres. J Biol Chem 276:32330–32337

Figure Legends

Fig. 1 Electron micrographs of WT Dp samples showing the effects of transverse tension and 1% Triton X-100 treatment. Dp samples without transverse tension or detergent treatment (**a**) failed to show filamentous architecture between the sarcolemma and peripheral myofibrils. The subsarcolemmal space (the space between the two *black open arrow*s) cannot be identified because the sarcolemma (three *black arrowheads*) remains closely attached to the peripheral myofibrils. When tension was applied without detergent treatment (**b**), the subsarcolemmal space (the space between the two *black open arrows*) could be identified between the sarcolemma (three *black arrowheads*) and peripheral myofibrils. Some filamentous structures could also be observed. Many membrane organelles of unknown origin (*white open arrowheads*) were still present, most likely because there was no detergent treatment. Dp samples subjected to 1% Triton X-100 without tension treatment (**c**) also failed to show filaments. Dp samples subjected to both 1% Triton X-100 and transverse tension treatment (**d**) provided better observations of the filamentous anchoring structures. Z, Z disk; M, M line.

Fig. 2 High-magnification electron micrographs of longitudinally sectioned WT Dp samples treated with transverse tension only. Three independent Dp samples (**a, b, c**) were used. The subsarcolemmal space could be observed between the sarcolemma (three *black arrowheads*) and peripheral myofibrils. The filamentous anchoring structures apparently survived the tension treatment. Transversely running thin filaments (*white arrow*) and 10-nm filaments (*black arrow*) could be identified. The thin filaments (white arrowheads) showed oblique elongation in the subsarcolemmal space and in the intermyofibrils. Subsarcolemmal densities (*white open arrows*) were found to be in direct contact with the filamentous structures. Organelles of unknown origin (*white open arrowheads*) were found in some locations. The *boxed areas* in **a, b,** and **c** are shown at a higher magnification (**d, e, f**). Length of the filament diameter was measured and then calculated to have the value of filament diameter. The space between two *white arrows* is 10 nm. In images **a, b,** and **c**, thin filaments (*white arrow)* were 8.20 ± 1.16 nm (n = 12) and 10-nm filaments (*black arrow*) were 11.65 ± 1.63 nm (n = 4). Z, Z disk; M, M line.

Fig. 3 Electron micrographs of transversely sectioned WT Dp samples treated with transverse tension only. These sections (**a, b**) confirmed the appearance of the filamentous anchoring structures connecting the sarcolemma (three *black arrowheads*) and peripheral myofibrils. Thin filaments (*white arrows*) were clearly observed to originate from the A-band (A), and some were observed to originate from the I-band (I). In both cases, the filaments were connected to the sarcolemma. Subsarcolemmal densities (*white open arrows*) were in direct contact with the filamentous structures. Membrane organelles of unknown origin (*white open arrowheads*) were observed between the structures. Filament diameter was measured in the samples (**a** and **b**), and the thin filaments (*white arrows*) were 8.29 ± 0.55 nm (n = 11). Z, Z disk.

Fig. 4 Electron micrographs of longitudinally sectioned WT Dp samples treated with 1% Triton X-100 and transverse tension. The subsarcolemmal spaces were clearly exposed in these three independent samples (**a, b, c**). The filamentous structures, thin filaments (*white arrows*) and 10-nm filaments (*black arrows*) formed firm transverse connections between the sarcolemma (three *black arrowheads*) and the Z disks (Z) and M lines (M) of peripheral myofibrils. Most of the longitudinal structures were elongated thin filaments (*white arrowheads*). Some subsarcolemmal densities (*white open arrows*) were observed, especially above the Z disk (Z) and M line (M) areas. Debris from membrane organelles (*white open arrowheads*) was present but less abundant. The persistent appearance of firm anchoring structures despite treatment with 1% Triton X-100 and transverse tension ascertained the existence of filamentous structures as transverse and longitudinal anchoring structures between the sarcolemma and peripheral myofibrils. The *boxed area* in **a** is shown at a higher magnification (**d**). Length of the filament diameter was measured and then calculated to have the value of filament diameter. The space between two *white arrows* is 10 nm. In images **a**, **b**, and **c**, thin filaments (*white arrows*) were 8.23 ± 0.44 nm (n = 9) and 10-nm filaments (*black arrows*) were 10.38 ± 0.52 nm (n = 8).

Fig. 5 Electron micrographs of WT Dp samples treated with 0.03% saponin and transverse tension. The subsarcolemmal space can be observed in these samples (**a, b**). The filamentous structures can be identified in longitudinal sections (**a**) and transverse sections (**b**). Thin filaments (*white arrows*) and 10-nm filaments (*black arrows*), which are clearly visible, form transverse connections between the sarcolemma (three *black arrowheads*) and the Z disk (Z) (**a**, **b**). The longitudinal structures appear to be elongated thin filaments (*white arrowheads*), which are located in the intermyofibrills (**a**). Some subsarcolemmal densities (*white open arrows*) and membrane organelles of unknown origin (*white open arrowheads*) were present. Filament diameter was measured in the samples (**a, b**); thin filaments (*white arrows*) were 7.69 ± 0.33 nm (n = 8) and 10-nm filaments (*black arrows*) were 10.00 ± 0.50 nm (*n* = 7).

Fig. 6 Electron micrographs of longitudinally sectioned *mdx* Dp samples treated with 1% Triton X-100 and transverse tension [**a, b (insert)**]. As with the WT Dp samples subjected to the same treatment, the subsarcolemmal space (the space between the two *black open arrows*) was clearly exposed (**a**). The filamentous anchoring structures had a distinct appearance in the *mdx* samples. There were fewer filamentous structures in the *mdx* Dp, and there were very few structures connecting the M line (M) to the sarcolemma (three *black arrowheads*). Some 10-nm filaments (*black arrow*) were present above the Z disk (Z) areas (**b [insert)**]. Subsarcolemmal densities (*white open arrows*) were observed. Debris from the membrane organelles of unknown origin (*white open arrowheads*) was present in some locations. Filament diameter was measured in the samples [**b (insert)**]; 10-nm filaments (*black arrow*) were 10 nm ($n = 2$).

Fig. 7 Schematic representation of the ultrastructural components of the costamere. Filamentous anchoring structures along with the subsarcolemmal densities and elongated thin filaments in the subsarcolemmal space are depicted as components of costameres. Filamentous anchoring structures are composed of actin and intermediate filaments. Subsarcolemmal densities appear in all three domains of costameres. Based on the present study, the filamentous structures depicted to be inserted into subsarcolemmal densities. Z-domains, M-domains, and L-domains are illustrated. At the Z-domains of costameres, actin and intermediate filaments appeared to cooperate to attach the Z disks of peripheral myofibrils to the sarcolemma. While at the M-domains of costameres, our results suggest that only intermediate filaments form the connections between the M lines of peripheral myofibrils and the sarcolemma. The subsarcolemmal densities in Z-domains and M-domains interact with integral membrane proteins (β-dystroglycans, sarcoglycans, integrin, etc). These proteins interactions continue to form a structural link by subsequently associate with suprasarcolemmal protein (α-dystroglycans, etc) and with the basal lamina proteins (laminin-2, etc). At the L-domains of costameres, elongated thin filaments extend from the peripheral myofibrils to the sarcolemma. Interaction between subsarcolemmal densities in L-domain with integral membrane protein is expected, but detail information is still unknown (dotted areas).

1 **Figures**

2 **Fig. 1**

Figure 1

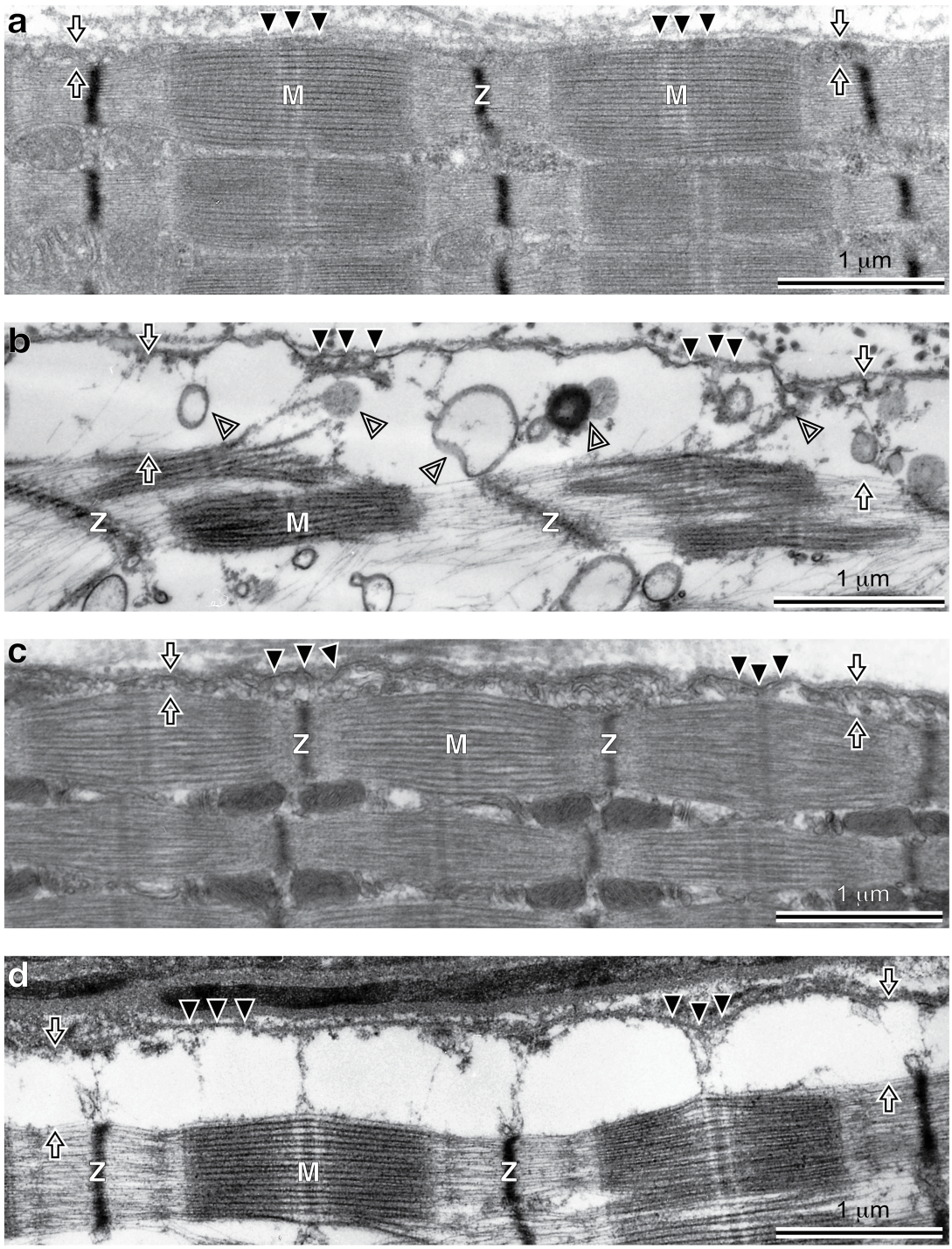

3

4

1 **Fig. 2**

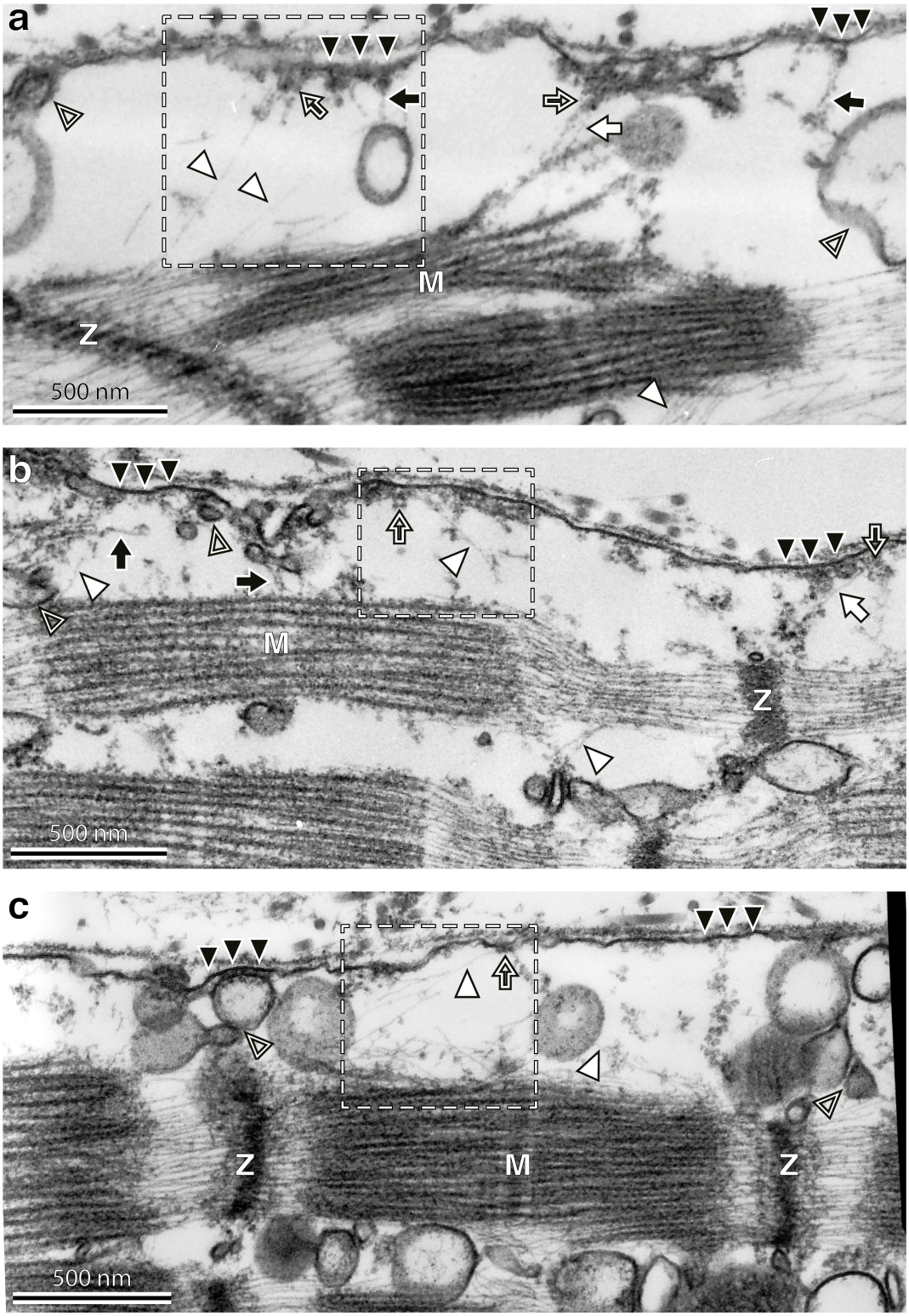

2

3

1 **Fig 2 (continued)**

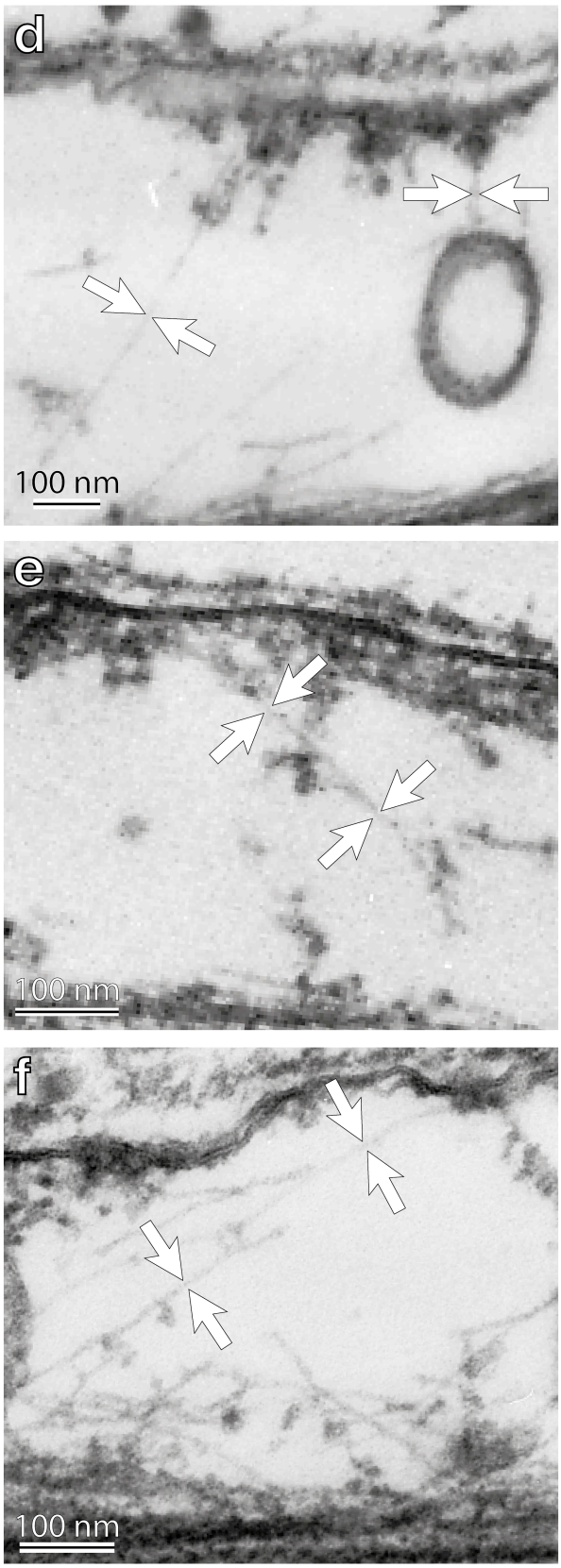

2

Fig. 3

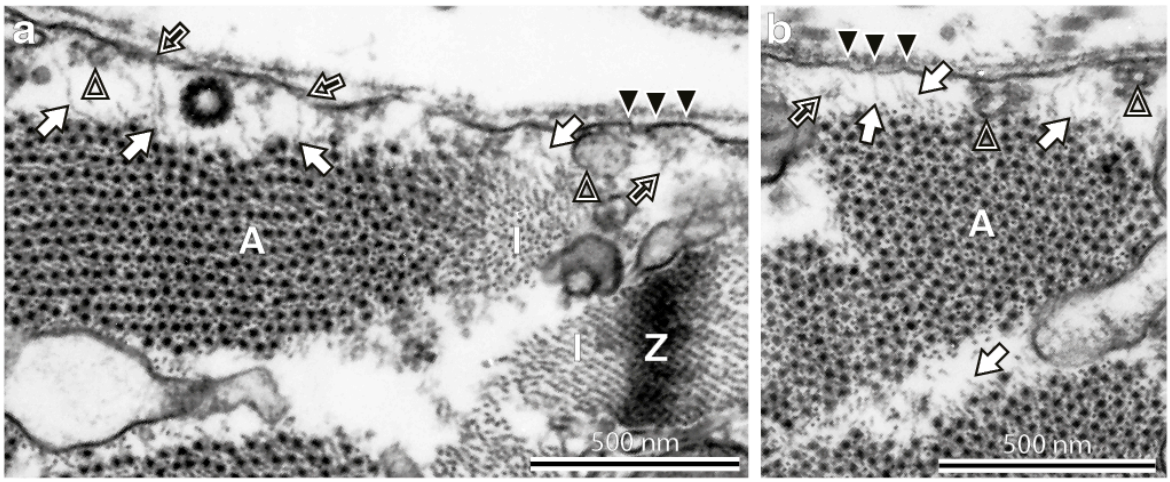

1 **Fig. 4**

Figure 4

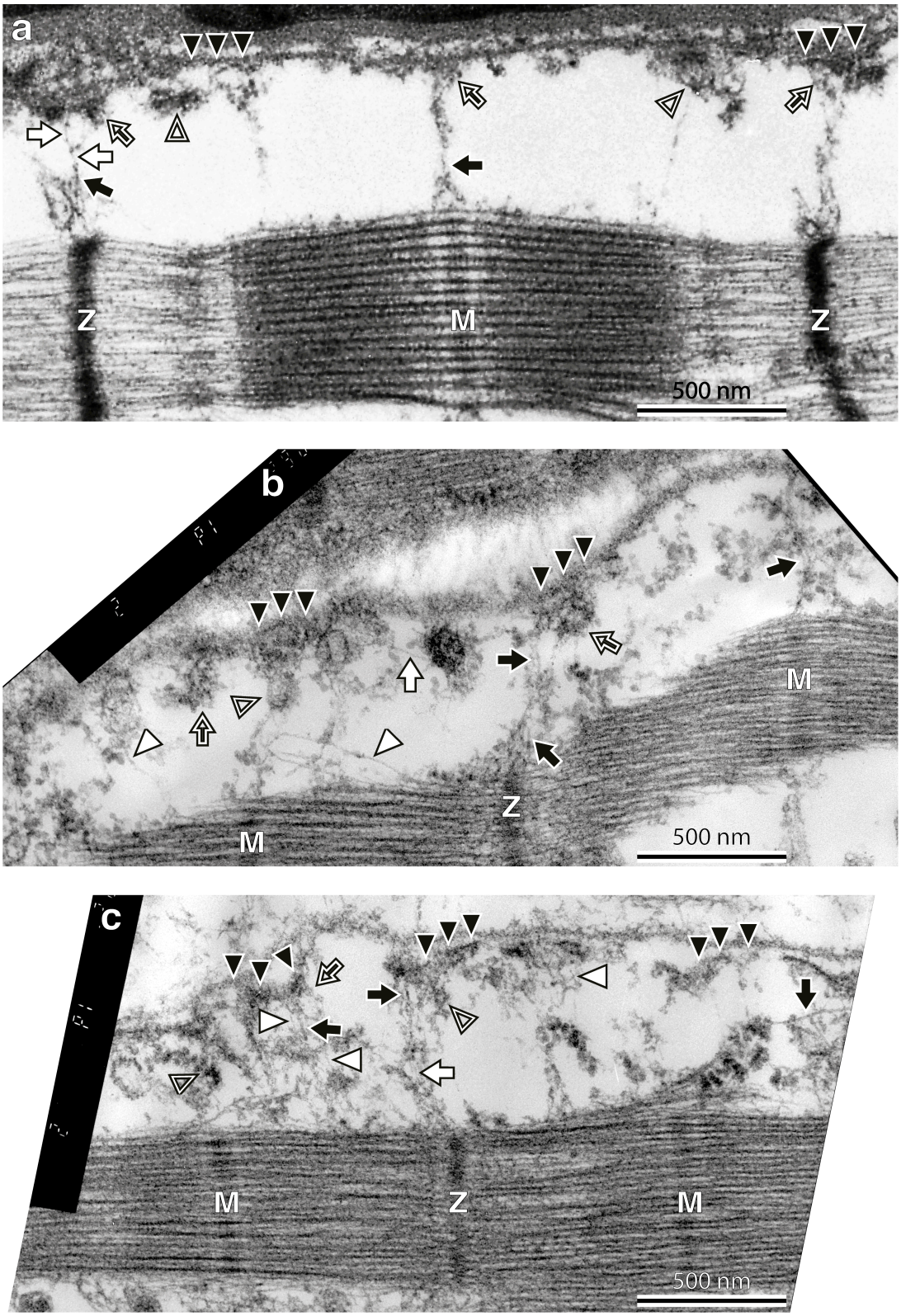

2

Fig. 4 (continued)

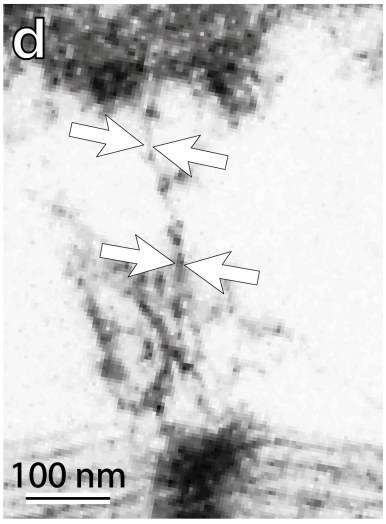

1 **Fig. 5**

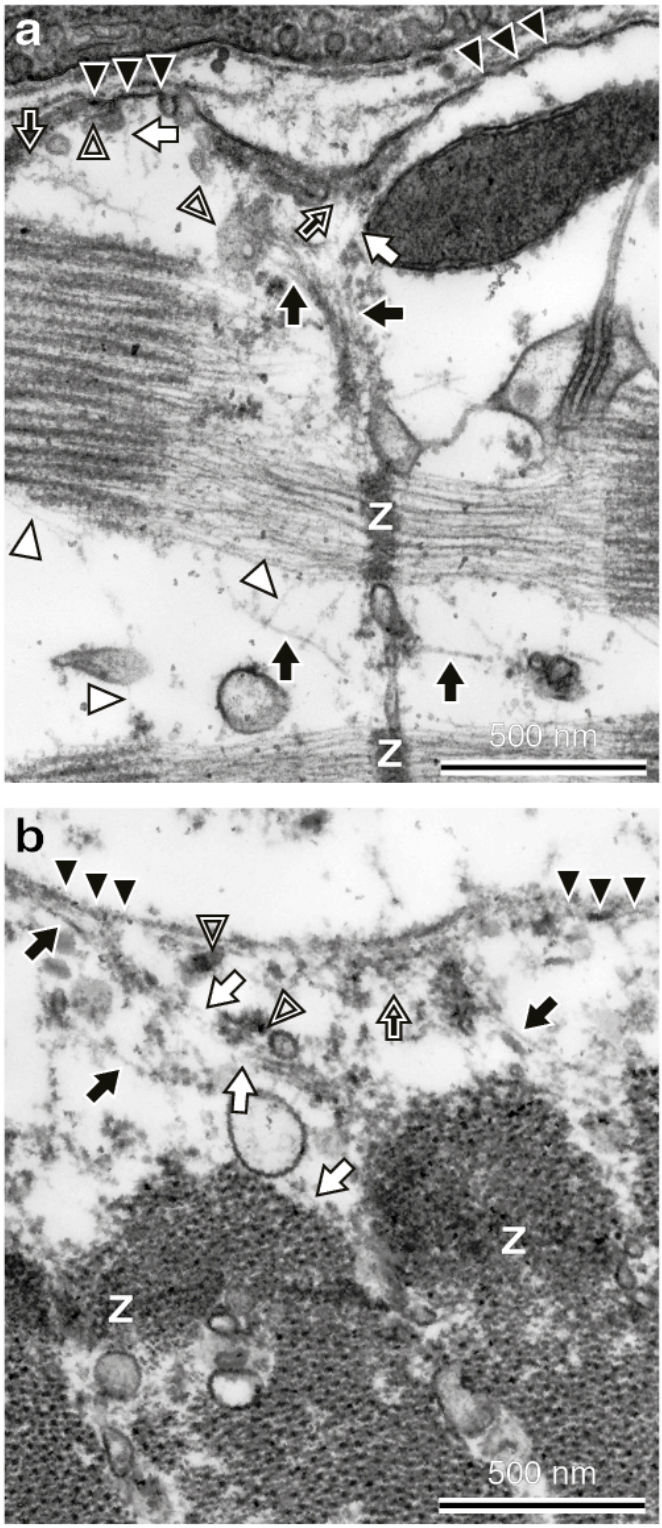

2

3

Fig. 6

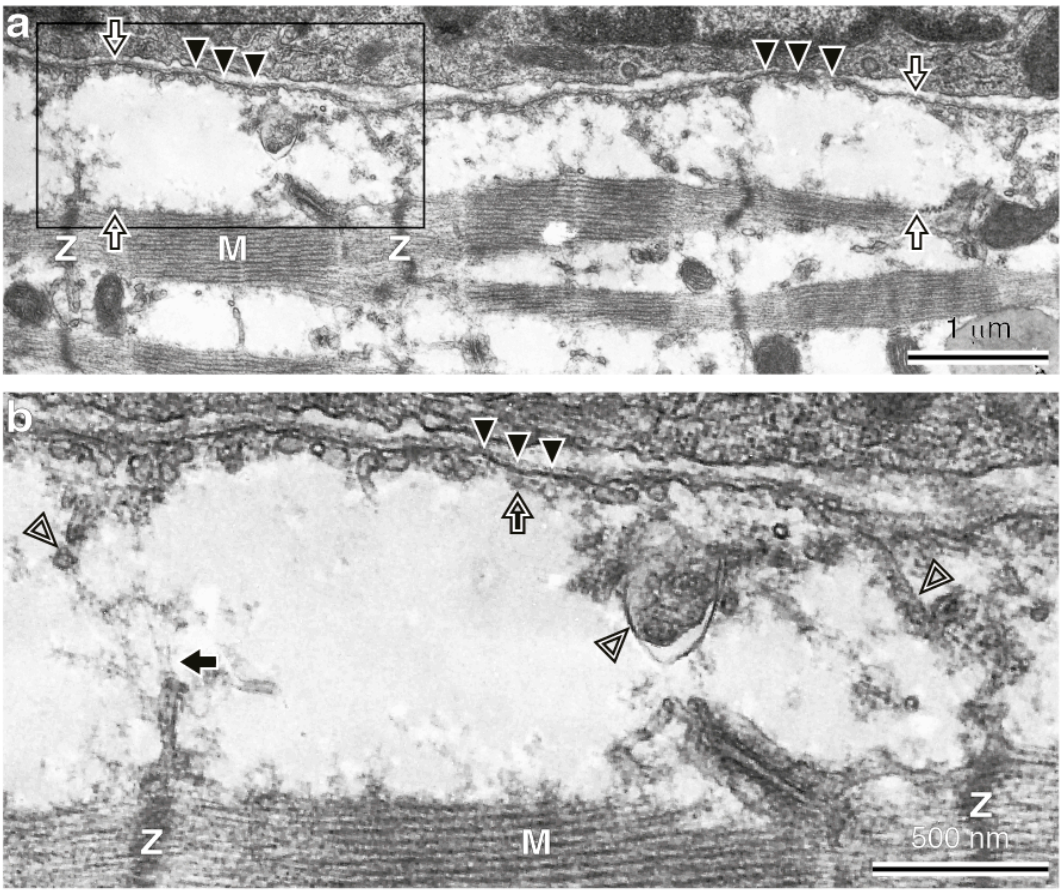

1 **Fig.7**

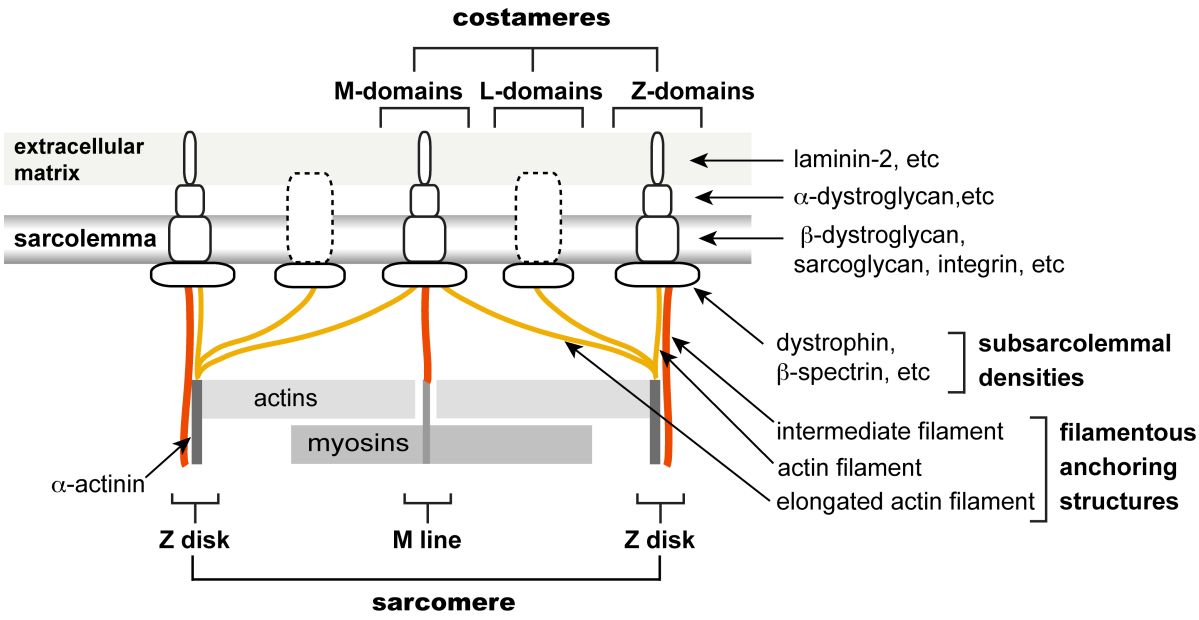
costameres
M-domains
L-domains
Z-domains
extracellular matrix
sarcolemma
laminin-2, etc
α-dystroglycan,etc
β-dystroglycan, sarcoglycan, integrin, etc
dystrophin, β-spectrin, etc
subsarcolemmal densities
actins
myosins
intermediate filament
actin filament
elongated actin filament
filamentous anchoring structures
α-actinin
Z disk
M line
Z disk
sarcomere

2